Jurnal Kejuruteraan 36(5) 2024: 2121–2127
https://doi.org/10.17576/jkukm-2024-36(5)-29

Simulation Study and Experimental Validation on The Effect of Generator Blade Type and Arrangement on Maximum Torque Generated For Micro Hydropower Generator

Mohd Haniff Hazmin* & Faizal Mustapha

Department of Aerospace Engineering, Faculty of Engineering,
Universiti Putra Malaysia, 43400 UPM Serdang, Selangor, Malaysia

**Corresponding author: haniff.hazmin@gmail.com*

Received 8 November 2023, Received in revised form 4 July 2024
Accepted 4 June 2024, Available online 30 September 2024

ABSTRACT

This paper contributes to an ongoing development of a micro hydropower network system tailored for implementation along river networks in Malaysia. The concept involves deploying multiple micro hydropower generators to charge a battery positioned on the riverbank. This interconnected hydropower network work alongside similar network systems to either charge larger batteries or serve multiple communities, enhancing its scalability and utility. The primary aim of this study is to determine a better generator blade type, and explore the relationship between the arrangement of generator blades in the river and the resulting torque generated. An experiment is conducted to determine the superior turbine type. The simulation process integrates engineering simulation software (ANSYS) and 3D modeling software (CATIA). ANSYS is employed to simulate river conditions with specific flow rates, while CATIA facilitates the design of generator blades, subsequently imported into ANSYS for simulation. The objective of the simulation is to identify the blade arrangement yielding the highest maximum generated torque. Subsequently, an experiment involving 3D printing the selected turbine types and measuring their rotational speed under consistent water flow conditions using a digital tachometer is conducted. From the experiment, it is found that curved blade types outperform straight blade types, while from the ANSYS simulation it is found that a distance between generator blades ranging from 300mm to 400mm offers optimal performance. This comprehensive approach enables a thorough evaluation of turbine configurations and their real-world performance, advancing micro hydropower technology for sustainable energy generation along river networks.

Keywords: hydropower, turbine, renewable energy, 3D printing, CATIA

INTRODUCTION

The waterwheel was once a common device used to convert potential energy from moving water into kinetic energy. This allowed people in the past to perform tasks such as milling flour, grinding wood, and pounding fibres (Nguyen et al. 2018; Viollet 2017). Nearly 100 years later, the development of water turbines during the Industrial Revolution completely replaced the use of waterwheels to drive electric generators (Warjito et al. 2019). This shift occurred due to the limitations of waterwheels, which are too large and restrict the flow rate and head that can be accumulated (Sritram & Suntivarakorn 2017).

Today, there are several turbine designs that fall into two types: reaction turbines and impulse turbines (Zaniewski et al. 2019). Reaction turbines need to be submerged in the water flow and enclosed to contain the water pressure. These turbines are driven by the moving water, which changes pressure as it flows through and transfers its energy to the turbines (Viollet 2017). One of the most popular reaction turbines is the Francis turbine, which is still widely used in many hydropower systems worldwide, especially in medium to high head sections (Zhang et al. 2023).

On the other hand, impulse turbines do not require encasement or submersion in water. They function by altering the velocity of a water jet, which applies pressure to the curved blades of the turbine, consequently altering the flow direction. This change in momentum generates a force on the turbine blades, causing the turbine to spin (Chitrakar et al. 2020). The Pelton Wheel is the most renowned design for impulse turbines, renowned for its high efficiency despite sharing a similar fundamental geometry to the traditional waterwheel (Ishola et al. 2019; Rafae Alomar et al. 2022).

In this study, a unique combination of the Tyson turbine and Straflo turbine is employed. The Tyson turbine represents a distinct hydropower system wherein a turbine is mounted beneath a raft or pontoon along the moving water and tethered to the shore or riverbank (Rachman 2011). The Tyson turbine does not need to be encased and is installed directly into the flowing water stream.

The Straflo turbine, a variant of the Kaplan turbine, integrates the generator along the circumference of the water channel, linked to the periphery of the runner (Singh & Prasad 2016). By combining and expanding both systems, the resultant system becomes more mobile, safer, and capable of accommodating considerable usage with an appropriate number of generators in place. This yields a series of Tyson-based hydropower systems. Each system incorporates a modified Straflo turbine to further enhance the power generation process. While this approach may generate less energy compared to conventional dams, the strategic networking of these innovative systems allows for the accumulation of generated energy, ultimately producing sufficient power with minimal environmental impact.

The experimental and simulation study conducted in this research aligns with another project focused on developing a small-scale hydropower generator tailored for remote areas in Malaysia. This hydropower generator initiative aims to bridge isolated regions with the modern world by providing electricity while simultaneously alleviating the country's overall electricity demand. Notably, the escalating electricity tariffs since 2014 highlight the costliness of supplying electricity to entire communities via the national main grid. (Ahmad et al. 2020). Given that many isolated communities are situated near rivers, this project serves as a valuable alternative power source, particularly during the rainy season when the risk of flooding escalates and solar panels are rendered less effective due to overcast skies. (Tun et al. 2018).

METHODOLOGY

In this study, several procedures are conducted to determine the desired specifications for the hydropower network system. Figure 1 shows the flow chart for the procedures involved. For this analysis, there are two types of turbine runner blades (curved blades and straight blades) considered for the analysis. Figure 2 shows both turbine runner blade types. These designs will undergo a fluid analysis to determine which blade type offers better potential for efficiency. Experimental analysis is conducted for both types of turbine runner blades to validate the fluid simulation findings. The analysis involves establishing an enclosed water flow system using water pumps and suspending the turbine runners in the water. A tachometer is employed to measure the rotation per minute (RPM) of the turbine runners. The turbine runners are fabricated via 3D printing based on the CATIA 3D models previously generated. Figure 3 depicts the setup of the enclosed system, accompanied by other tools and materials as labelled.

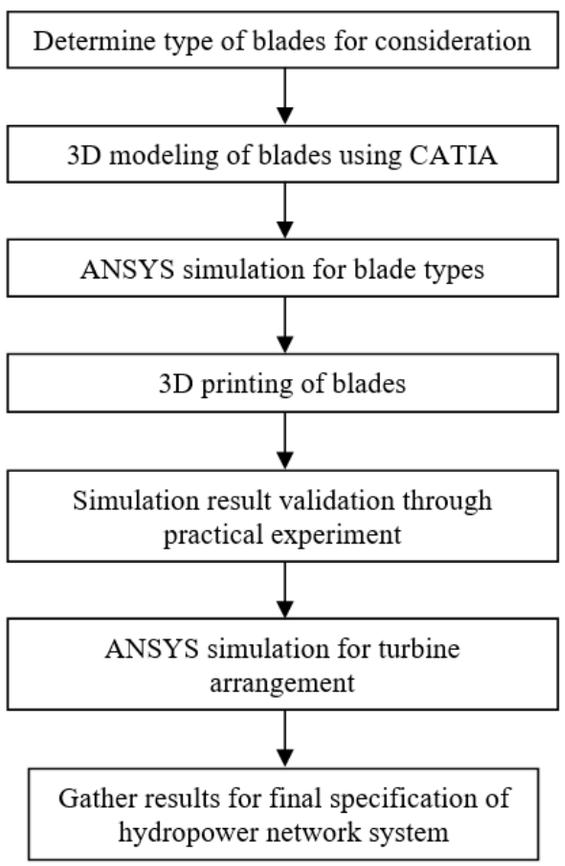

FIGURE 1. Flowchart

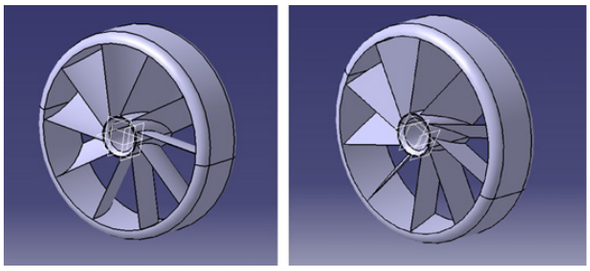

FIGURE 2. Turbine runner with curved blades (left) and turbine runner with straight blades (right)

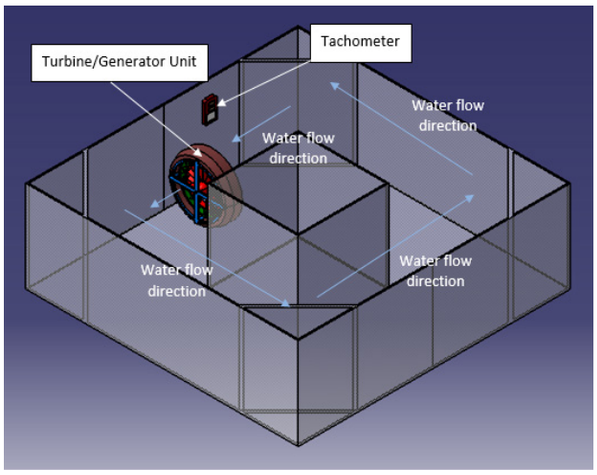

FIGURE 3. Setup for experimental turbine blade analysis

In this experiment, a strip of reflective tape is affixed to a small area on the outer circumference of the turbine runner. This tape allows the laser from the tachometer to accurately determine the RPM. The turbine runner is suspended on a shaft held in position by several fishing lines. Two sets of experiments are conducted for each turbine runner: the first set employs one water pump, while the second set utilizes two water pumps. This variation in the number of water pumps allows for the collection of more data to enhance accuracy. Each set comprises three repetitions, with the average of the three measurements calculated. During each repetition, the turbine is allowed to spin briefly until it reaches a stable rotation, and the RPM reading is then taken. This ensures consistent and precise readings. The turbine exhibiting the highest overall RPM progresses to the subsequent analysis. Figure 4 illustrates an example of how the reading is measured using the tachometer. As previously mentioned, the new hydropower generator system will comprise a combination of a Tyson-based system and a modified Straflo turbine. In practical application, permanent magnets will be affixed to the outer circumference of the turbine runners. These turbine runners will move laterally with stator coils, which will be positioned on the inner circumference of the turbine casing. The scaled prototype of the turbine runner has a diameter of 150mm and a thickness of 50mm. The assembled scaled prototype for the hydropower generator unit is depicted in Fig. 5.

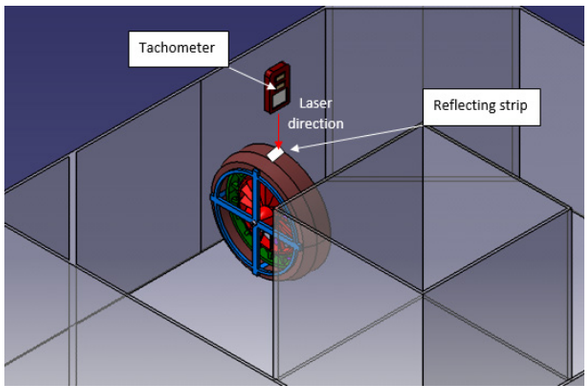

FIGURE 4. Example of a reading measurement using a laser tachometer

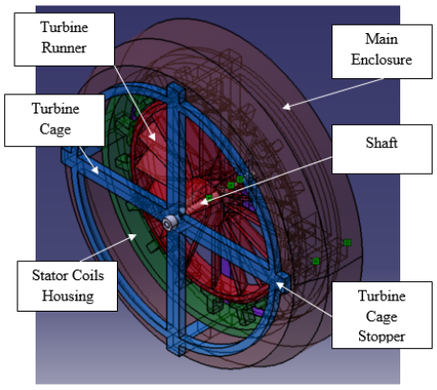

FIGURE 5. Assembled scaled hydropower generator unit prototype

The chosen turbine runner from the previous analysis is arranged as shown in Fig. 6. The X, Y and Z axis are represented by the white lines labeled correspondingly.

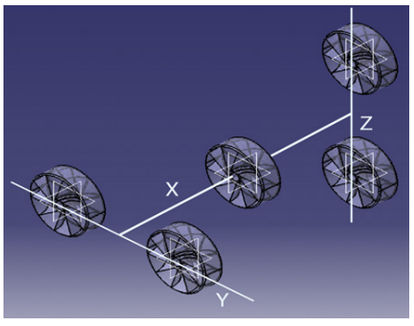

FIGURE 6. Turbine arrangement with axis shown

In this analysis, the distance between the centres of the turbines on the Y-axis starts at 200mm (Y value), while the distance between the centres of the turbines on the Z-axis also begins at 200mm (Z value). The distance between turbines on the Z-axis and the turbine in the middle of the X-axis starts at 0mm (X value), which remains consistent for turbines on the Y-axis to the turbine in the middle of the X-axis.

The simulation is divided into 3 parts, where part 1 involves increasing X value from 0mm to 500mm with a constant Y and Z value at 200mm. Part 2 involves repeating the steps in part 1 but with Y and Z values at 300mm. Part 3 involves repeating the steps in part 1 but with Y and Z values at 400mm. The limit is set at 400mm since the product will have limited space to operate and simplify installation.

After arranging the turbine runners using CATIA, the 3D models are exported into ANSYS for simulation. In ANSYS, an enclosure is created around the turbine runners to simulate a section of a river. A suitable mesh is generated, and input and output for the river water flow are assigned to the appropriate locations of the enclosure. Simulation conditions, such as river flow rate and material properties, are specified in ANSYS. For this simulation, a river flow rate of 0.5833 ms^{-1} is utilized, obtained from a previous hydropower assessment study conducted on local rivers. (Gasim et al. 2013).

The flow contours for each analysis are subsequently examined to understand how the river water flow interacts with the turbine runners. By utilizing the built-in calculator within the result window, the maximum torque for each analysis on each turbine runner is determined and documented.

RESULTS AND DISCUSSION

Examples of velocity contours from the simulation are illustrated in Fig. 7 and Fig. 8. Figure 9 shows the result of the fluid analysis on a straight blade turbine runner, while Fig. 10 shows the result for a curved blade turbine runner. Based on the analysis results, the pressure accumulated on the turbine runner with curved blades reached 1.33147 Pa, significantly higher than the pressure on the turbine runner with straight blades, which measured at 0.204002 Pa. This indicates that the turbine runner with curved blades has the potential to rotate at a higher RPM compared to the turbine runner with straight blades under the same river velocity. Table 1 presents the experimental results for turbine runners with curved blades and straight blades.

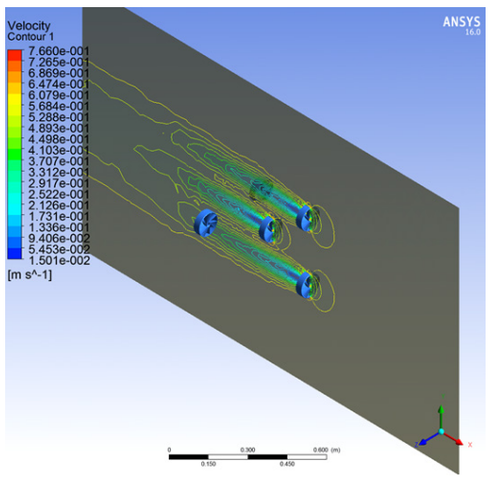

FIGURE 7. Velocity contour on XY plane

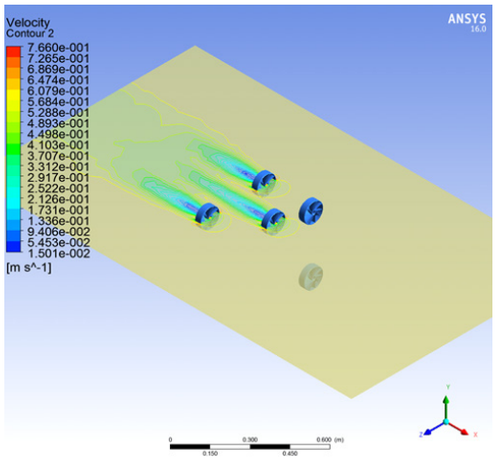

FIGURE 8. Velocity contour on XZ plane

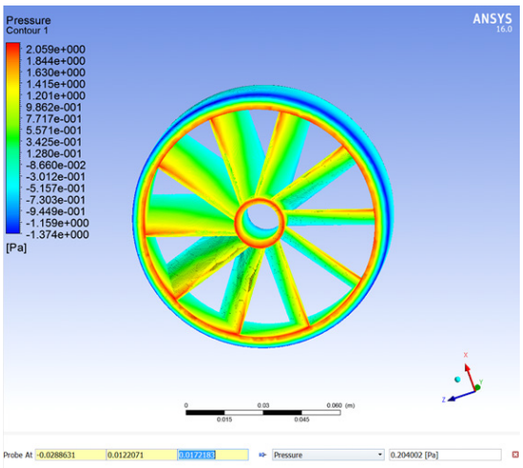

FIGURE 9. Pressure contour for straight blade turbine runner

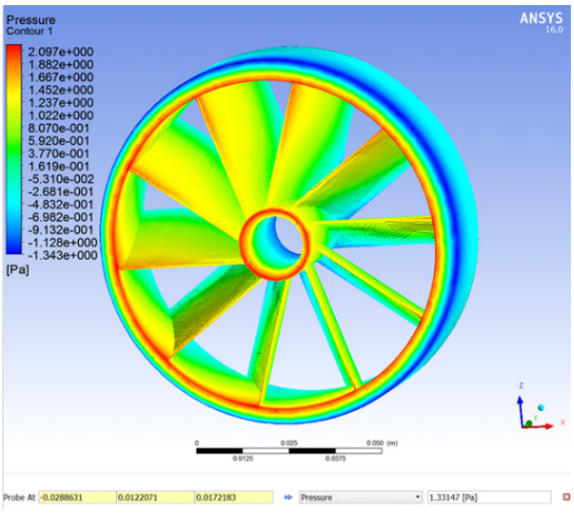

FIGURE 10. Pressure contour for curved blade turbine runner

TABLE 1. RPM readings of turbine runners

Run	Curved Blades		Straight Blades	
	RPM with 1 Water Pump	RPM with 2 Water Pumps	RPM with 1 Water Pump	RPM with 2 Water Pumps
1	12	35	9	25
2	12	33	11	27
3	14	35	8	27
Average	12.667	34.333	9.333	26.333

Table 1 demonstrates a significant difference in rotational performance between the turbine runner with curved blades and its straight-bladed counterpart. The turbine runner with curved blades exhibits a 35.7% performance advantage over the straight-bladed version when operated with a single water pump, and a 30.4% advantage when operated with two water pumps. These findings consistently favour the turbine runner with curved blades across both scenarios.

TABLE 2. Maximum torque generated on each turbine runners

Y, Z (mm)	X (mm)	T1 (Nm) ($\times 10^{-4}$)	T2 (Nm) ($\times 10^{-4}$)	T3 (Nm) ($\times 10^{-4}$)	T4 (Nm) ($\times 10^{-4}$)	T5 (Nm) ($\times 10^{-4}$)	Total T (Nm) ($\times 10^{-4}$)
	0	3.74082	3.74536	3.74722	3.74715	3.73372	18.71427
	100	3.00482	3.01700	3.56108	3.53117	3.55106	16.66513
	200	3.00446	3.00325	3.51109	3.41034	3.50976	16.43890
	300	2.95445	2.9654	3.54727	3.36985	3.54289	16.37986
	400	2.93042	2.90152	3.55828	3.32846	3.54806	16.26674
200	500	2.81107	2.84464	3.56912	3.31251	3.56227	16.09961
	0	3.71530	3.71427	3.73100	3.79215	3.70916	18.66188
	100	3.61434	3.60062	3.64046	3.67228	3.64495	18.17265
	200	3.55679	3.54404	3.59844	3.59844	3.58204	17.87975
	300	3.54020	3.53566	3.57207	3.53621	3.54510	17.72924
	400	3.52737	3.51282	3.56705	3.52727	3.54501	17.67952
300	500	3.51282	3.50704	3.57556	3.53588	3.55759	17.68889
	0	3.70443	3.68658	3.72847	3.75420	3.70182	18.57550
	100	3.64967	3.65416	3.66140	3.68531	3.62466	18.27520
	200	3.62104	3.61649	3.61035	3.60657	3.57534	18.02979
	300	3.62213	3.57580	3.60789	3.60120	3.57861	17.98563
	400	3.58866	3.58697	3.57713	3.58498	3.57308	17.91082
400	500	3.58157	3.57608	3.58764	3.58537	3.58780	17.91846

Table 2 presents the detailed results for turbine runners with curved blades in each ANSYS simulation analysis on the relationship between turbine arrangements and accumulated torque generation. Additionally, Figure 11 illustrates the relationships between X, Y, and Z values, and the maximum torque generated. Furthermore, Figure 15 offers a comparison of the relationship between Y and Z values of 200mm, 300mm, and 400mm, and the maximum torque.

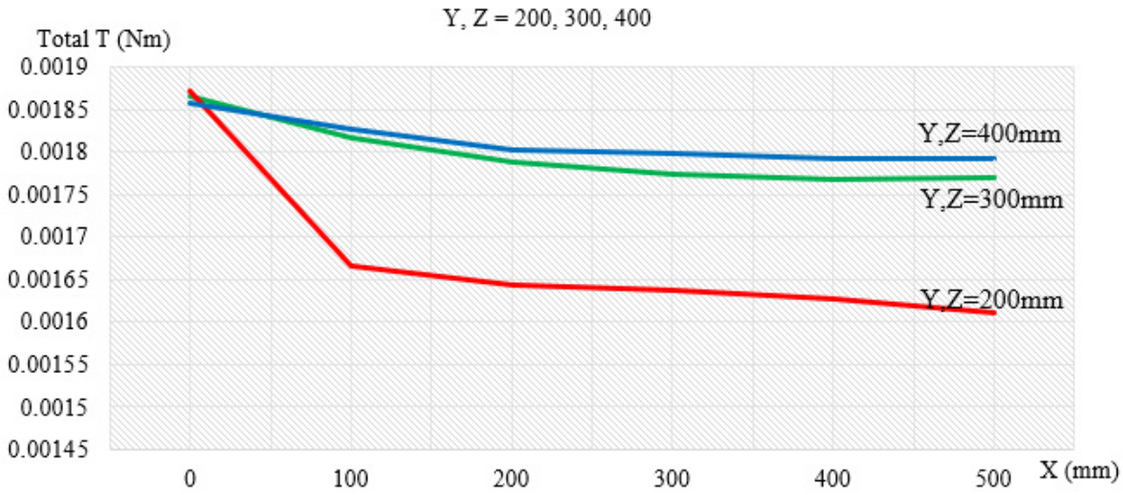

FIGURE 11. Relationship between Y and Z values of 200mm, 300mm and 400mm, and the maximum torque

From Figure 11, it is evident that the maximum torque increases with higher Y and Z values. Notably, there's a significant difference observed at Y and Z values of 200mm compared to 300mm and 400mm. This disparity may stem from the constrained water flow at Y and Z values of 200mm due to the closer proximity of the turbine runners. As the turbine runners become more spaced out, such as at Y and Z values of 300mm, the water flow can distribute more evenly and recover from its turbulent state, resulting in improved rotations.

Additionally, from Figure 11 the parameter X also plays a significant role in determining the generated torque. When X = 0, the torque reaches its peak because the water flow impacting the entire turbine maintains its initial potential energy. However, employing an arrangement with X = 0 substantially reduces water velocity due to the limited space between the initial wall-like arrangement of turbine runners. Consequently, the water flow may not have sufficient energy to rotate the subsequent turbine runners effectively. While this arrangement may yield superior results in terms of torque generation, it may not be practical for environments utilizing multiple similar turbine arrangements.

It is recommended to further investigate water flow dynamics across arrangements with multiple turbine runners. Additionally, conducting experiments with larger-scale water flow systems could provide more practical insights into rotational performance, aiding in the determination of an optimized X value for Malaysian river conditions.

While certain arrangements may yield promising results in simulations, they also may not be practical for real-world applications involving multiple similar turbine arrangements. For future enhancements, employing more precise simulations with enhanced computational capabilities can provide deeper insights into water flow dynamics. This, coupled with experiments utilizing larger-scale water flow systems, can refine the optimization of X values, contributing to the development of the most effective turbine runner arrangement.

CONCLUSION

It is clear that adopting a more spaced-out turbine arrangement can result in higher total torque values, a significant advantage for a hydropower generator. Optimal clearance between turbines, typically ranging from 300mm to 400mm along the X, Y, and Z axes, yields a favourable torque range. However, a constraint on the lateral distance between turbine runners becomes necessary as rivers do not offer infinite space. This limitation is essential to streamline installations and minimize the utilization of river space, ensuring that other users such as humans and animals can freely access and utilize the river.

ACKNOWLEDGEMENT

The author would like to thank the Department of Aerospace Engineering, Faculty of Engineering, Universiti Putra Malaysia for providing the opportunity for this research.

DECLARATION OF COMPETING INTEREST

None.

REFERENCES

Ahmad, N. A., Hussain, N. H., Anas, N. & Jamian, J. J. 2020. Pemasangan panel solar bagi menampung bekalan elektrik tambahan untuk institusi pendidikan agama persendirian di luar bandar: melalui pendekatan program kemasyarakatan komuniti. *Malaysian Journal of Sustainable Environment* 7(2): 161–184. https://doi.org/10.24191/myse.v7i2.10270

Bretheim, J., Bardy, E., College, G. C. & City, G. 2012. A review of power-generating turbomachines. *Proceedings of the 2012 ASEE North Central Section Conference* 1–15. https://web.itu.edu.tr/aydere/review.pdf

Chitrakar, S., Solemslie, B. W., Neopane, H. P. & Dahlhaug, O. G. 2020. Review on numerical techniques applied in impulse hydro turbines. *Renewable Energy* 159: 843–859. https://doi.org/10.1016/j.renene.2020.06.058

Gasim, M. B., Toriman, M. E., Idris, M., Lun, P. I., Kamarudin, M. K. A., Nor Azlina, A. A., Mokhtar, M. & Mastura, S. A. S. 2013. River flow conditions and dynamic state analysis of Pahang river. *American Journal of Applied Sciences* 10(1): 42–57. https://doi.org/10.3844/ajassp.2013.42.57

Georgescu, A. & Georgescu, S. 2007. *Hidraulica retelelor de conducte si Masini hidraulice* (Hydraulics of Piping Networks and Hydraulic Machinery). Editura Printech.

Ishola, F. A., Kilanko, O. O., Inegbenebor, A. O., Sanni, T. F., Adelakun, A. A. & Adegoke, D. D. 2019. Design and performance analysis of a model pico size pelton wheel turbine. *International Journal of Civil Engineering and Technology (IJCIET)* 10(5): 727–739.

Nguyen, M. H., Jeong, H. & Yang, C. 2018. A study on flow fields and performance of water wheel turbine using experimental and numerical analyses. *Science China Technological Sciences* 61(3): 464–474. https://doi.org/10.1007/s11431-017-9146-9

Pelton, L. A. 1880. *Water Wheel* (Patent No. US233692). United States Patent Office. October 26, 1880. Application filed July 3, 1880. https://patentimages.storage.googleapis.com/6a/19/4e/26608eb3abf576/US233692.pdf

Rachman, A. & Tambi. 2011. Reviews: Pontoon, an alternative flexible cheap mounting option for the renewable decentralized river current turbine power service. *Journal of Metropilar Haluoleo University* 9: 203–208.

Rafae Alomar, O., Maher Abd, H., Mohamed Salih, M. M. & Aziz Ali, F. 2022. Performance analysis of Pelton turbine under different operating conditions: An experimental study. *Ain Shams Engineering Journal* 13(4): 101684. https://doi.org/10.1016/j.asej.2021.101684

Singh, A. & Prasad, V. 2016. Design and performance analysis of straflo turbine using CFD. *IOSR Journal of Mechanical and Civil Engineering (IOSR-JMCE)* 13(4): 54–59. https://doi.org/10.9790/1684-1304035459

Sritram, P. & Suntivarakorn, R. 2017. Comparative Study of Small Hydropower Turbine Efficiency at Low Head Water. *Energy Procedia* 138: 646–650. https://doi.org/10.1016/j.egypro.2017.10.181

Tun Jamil, S. J., Ahmad, N. A. & Jasiman, J. J. 2018. Connecting felda communities with solar electrification during flood disaster: the methodology. *Malaysian Journal of Sustainable Environment* 4(1): 57–76. https://doi.org/10.24191/myse.v4i1.5607

Viollet, P. L. 2017. From the water wheel to turbines and hydroelectricity. Technological evolution and revolutions. *Comptes Rendus - Mecanique* 345(8): 570–580. https://doi.org/10.1016/j.crme.2017.05.016

Warjito, Adanta, D., Budiarso, Nasution, S. B. S. & Kurnianto, M. A. F. 2019. The effect of blade height and inlet height in a straight-blade undershot waterwheel turbine by computational method. *CFD Letters* 11(12): 66–73. https://doi.org/10.3390/pr11051502

Zaniewski, D., Klimaszewski, P., Witanowski, Ł., Jędrzejewski, Ł., Klonowicz, P. & Lampart, P. 2019. Comparison of an impulse and a reaction turbine stage for an ORC power plant. *Archives of Thermodynamics* 40(3): 137–157. https://doi.org/10.24425/ather.2019.129998

Zhang, T., He, G., Guang, W., Lu, J., Song, X., Zhu, D. & Wang, Z. 2023. Investigation of the Internal Flow in a Francis Turbine for Comparing the Flow Noise of Different Operation Conditions. *Water (Switzerland)* 15(19): 1–14. https://doi.org/10.3390/w15193461